Phase behaviour of the solid proton conductor $CsHSeO_4$

2008 J. Phys.: Condens. Matter 20 365218

(http://iopscience.iop.org/0953-8984/20/36/365218)

J. Phys.: Condens. Matter **20** (2008) 365218 (8pp) doi:10.1088/0953-8984/20/36/365218

Phase behaviour of the solid proton conductor $CsHSeO_4$

E Ortiz[1], J C Tróchez[1] and R A Vargas[2]

[1] Department of Physics, Universidad del Atlántico, AA 1890, Barranquilla, Colombia
[2] Department of Physics, Universidad del Valle, AA 25360, Cali, Colombia

E-mail: eortiz@uniatlantico.edu.co, eortizmunoz@hotmail.com, jtrochez@uniatlantico.edu.co and rvargas@univalle.edu.co

Received 4 June 2008
Published 19 August 2008
Online at stacks.iop.org/JPhysCM/20/365218

Abstract
The previously found phase transitions in $CsHSeO_4$ at around 80 and 128 °C were carefully examined by using simultaneous thermogravimetric and differential scanning calorimetric analysis, modulated and conventional differential scanning calorimetric analysis, impedance spectroscopy, and x-ray diffraction. Our results show evidence that at these transition temperatures, dehydration processes take place at or very near the surface of the crystal. As a consequence, our results support the assertion that the $CsHSeO_4$ phase above 128 °C is not a superprotonic conducting phase, but rather a $Cs_2Se_2O_7$–H_2O system that grows over $CsHSeO_4$. The water strongly bound to the dimer dissolves part of the surface salt, providing protons and other ions such as Cs^+ that transport charge through the water embedded in the dimer matrix.

1. Introduction

Generally, for technical reasons, a solid electrolyte instead of a liquid one is preferred for fuel cell applications. Proton-conducting polymer electrolyte membranes are not truly solid phases because they contain liquid-like regions between the polymer molecules, and do not conduct protons exclusively [1]. Alternatively, solid acids (true solid proton conductors [1]) have been proposed as fuel cell electrolytes [2–4]. These salts are comprised of oxyanions—such as SO_4 and SeO_4—linked together via hydrogen bonds. For example, some $MHXO_4$ (M = Cs, NH4, Rb; X = S, Se) compounds have been suggested for full cell applications [2–4], because at high temperatures they undergo a superionic (also called superprotonic) phase transition [5, 6].

In 1982, Baranov *et al* [5] discovered that upon heating $CsHSO_4$ (CHS) and $CsHSeO_4$ (CHSe) through 141 and 125 °C, respectively, their conductivity values increase by several orders of magnitude to 10^{-2} and 10^{-3} S cm^{-1}, in that order. A transition to a superionic conducting phase was claimed for both compounds at these temperatures. However, on the cooling runs to room temperature they did not return to the values observed when the salts were first heated; instead, for both solid acids, they were around half an order of magnitude higher.

For CHS and CHSe, aside from this class of phase transitions, there is another one that is quite accepted. Hereinafter, we will refer to its room, intermediate, and high temperature (the superionic conducting one) phases as the III, II and I phases, respectively. Even though the object of this work is to study the phase behaviour of CHSe above room temperature, we will frequently refer to CHS because its physical and chemical room and high temperature properties behave in much the same way as those of CHSe. At room temperature, the phase III of CHSe has a monoclinic symmetry with space group $P2_1/c$, and its structure consists of zigzag chains of hydrogen bonds along the c axis of the crystal, linking the SeO_4 tetrahedra [7, 8], just like the CHS room temperature phase structure except that chains go along the b axis [9]. On heating, according to some authors, at some temperature between 50 and 97 °C a phase transition occurs (III → II). This wide spread in the reported transition temperatures can be reviewed as follows: by using Brillouin spectroscopy, Luspin *et al* [10, 11] reported the transition at 50 °C; depending on the thermal history of the sample, the differential scanning calorimetric analysis of Pham-Thi *et al* [12] and Colomban *et al* [13] measured the transition at 70 ± 20 °C; using the last technique Baranowski *et al* [14] observed the first-order phase transition at 82 ± 3 °C; and 'in certain cases' by using conductivity measurements, Baranov *et al* [5] monitored the transition at 97 °C. Similarly, the reported III → II phase transition temperature for CHS also has considerable spread: from 57 to 97 °C [15].

On the other hand, by using neutron diffraction studies, Belushkin *et al* [16] found that when CHSe is heated from below room temperature, diffraction spectra start to change at 87 °C and a complete rearrangement of the spectra takes place at 127 °C. Further heating up to 152 °C does not change the spectra. This observation allows confirming that a structural phase transition on this salt starts at temperatures as low as 87 °C and it is much extended in temperature, finishing at 127 °C. Therefore, these authors concluded that between these temperatures there is a two-phase system. Additionally, by using infrared spectroscopy, De Sousa *et al* [17] showed that the 80–128 °C temperature range is characterized by the coexistence of the room temperature modes (modes of phase III) and some modes of the superprotonic conducting phase (modes of phase I): upon heating the salt through this temperature range, while the dielectric strength of the phase III modes abruptly falls until 128 °C is reached (e.g. the 720 cm^{-1} mode) the emergent mode situated at 670 cm^{-1} behaves in the opposite manner. The authors associated the 720 cm^{-1} and 670 cm^{-1} modes with a stretching motion of the Se–OH mode involved in the $(HSeO_4^-)_n$ chain and a stretching motion of $(HSeO_4^-)_2$ dimers, respectively. The latter are formed when the H-bond breaking (proton diffusion) appears. In the light of their result, they conclude that the intermediate regime between 80 and 128 °C is a prelude to the transition to the superionic conducting phase (phase I) and that it is neither a new phase nor a coexistence of two phases.

If a CHSe sample is heated thought the III → II phase transition temperature and then cooled down to room temperature, the inverse transition does not occur, but if a proper contact with water vapour and mechanical (gridding or one-dimensional pressure) treatment is applied the II → III phase transition is induced [14, 18]. This phenomenon also occurs for CHS [18, 19]. According to these works, water probably plays the role of a molecular lubricant, which facilitates the inverse transition [14]. On the other hand, from neutron scattering studies, Belushkin *et al* [16] showed that if a fresh CHSe sample is heated to 152 °C (some degrees above the temperature range where the salt is a two-phase system) and then cooled down to room temperature, the sample is the two-phase system and the inverse transformation to the stable phase III at this temperature does not occur, even if it is kept at this temperature for a four-week period. In contrast, according to Colomban *et al* [22], if CHSe is cooled from phase II or I down to room temperature and if it is annealed for some time (from three hours to many days) at this temperature, phase I can be obtained.

When CHSe is heated through given temperature, T_c, between 124 and 131 °C, a phase transition to the superprotonic conducting phase (phase I) takes place. As in the case for the III → II phase transition, the temperature value of this transition reported in the various papers does not coincide [5, 20–24].

With respect to the structure of phase I there are also discrepancies: according to Foose and Mitra [23], their differential thermal analysis revealed peaks at 127, 248, and 400–470 °C but no stable phase transformations were detected by x-ray analysis; further x-ray and optical studies by Yokota [24] showed that CHSe undergoes an improper ferroelastic phase transition at $T_c = 128$ °C to a phase with a tetragonal symmetry with cell parameters $a = b = 4.18$ Å and $c = 7.20$ Å. However, Yokota was unable to determine the space group of phase I (probably $4/mmm$ or $4/m$); according to Balagurov *et al* [25] the space group of this phase is probably $I4_1/amd$ (the same as was reported for the tetragonal symmetry of the CHS phase I [9]) but their cell parameters ($a = b = 5.906$ Å, $c = 14.43$ Å) do not coincide with those of Yokota [24].

Baranov *et al* [6] have proposed a model to explain the extraordinary conductivity increases that CHSe and CHS present when heated through T_c: the rise of the crystal symmetry under the phase transition from the low to the high conductivity phase leads to a rise of multiplicity of crystallographic proton positions, so the number of the structurally equivalent proton sites exceeds the number of protons in the unit cell and this proton disorder leads to the superprotonic conducting phase. This model does not require reorientational motion of $HSeO_4^-$(HSO_4^-) groups of CHSe (CHS) [6], as another one does [13, 16, 17]. According to Colomban [22], the (first-order [26]) II → I phase transition leads to a highly disordered plastic phase and the vibrational spectrum of phase I, similar to that of CHS, shows a 'quasi-liquid' state where proton, $(SeO_4)^{2-}$ ion and Cs^+ ion disorder contributes to the unusually high conductivity. Moreover, CHS and CHSe exhibit protonic and ionic conductivity above T_c but the drastic conductivity increase at the II → I is due principally to Cs^+ translational disorder [13]. Recently, ^{1}H NMR and ^{77}Se NMR measurements [27, 28] on CHSe have provided evidence of mobile protons and reorientational motion of the SeO_4 tetrahedron below T_c.

Like for CHS [21] in its plastic superionic conducting phase, when CHSe is observed under a polarization microscope, it shows colour patterns unusual for monocrystals [21].

When CHSe is further heated, thermal decomposition begins at around 207 °C [5], close to the onset temperature of decomposition for CHS (203 °C) [12]. It was also found that CHS decomposes according to the reaction

$$2CsHSO_4 \rightarrow Cs_2S_2O_7 + H_2O \qquad (1)$$

[12, 29, 30] and, conversely, $Cs_2S_2O_7$ is hydrolysed in the presence of water into $CsHSO_4$.

By using thermogravimetric analysis, mass spectroscopy, differential scanning calorimetric analysis, ac calorimetry, impedance spectroscopy, and x-ray diffraction we have shown that both the III → II and the II → I phase transitions of CHS do not take place [31]. We believe that the endothermic effects and conductivity changes associated with these transitions are due to chemical decomposition processes following reaction (1) at or very near the surface of the specimen.

Taking into account the fact that the physical and chemical room and high temperature properties of CHS and CHSe are so similar, the purpose of this work is to ascertain whether when CHSe is heated above room temperature, it really undergoes the III → II and II → I phase transitions or instead behaves as CHS does [31].

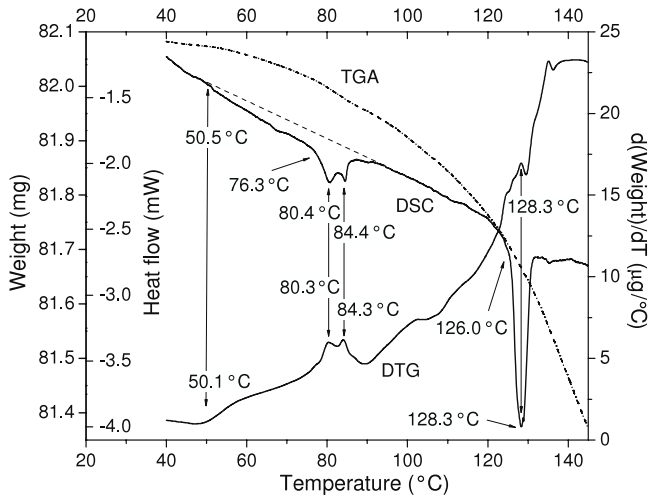

Figure 1. Simultaneous TGA–DSC measurements on a fresh dry CHSe sample in the 40–145 °C temperature range. The heating rate was fixed at 0.2 °C min^{-1}. The DTG curve corresponds to the temperature derivative of the TGA curve.

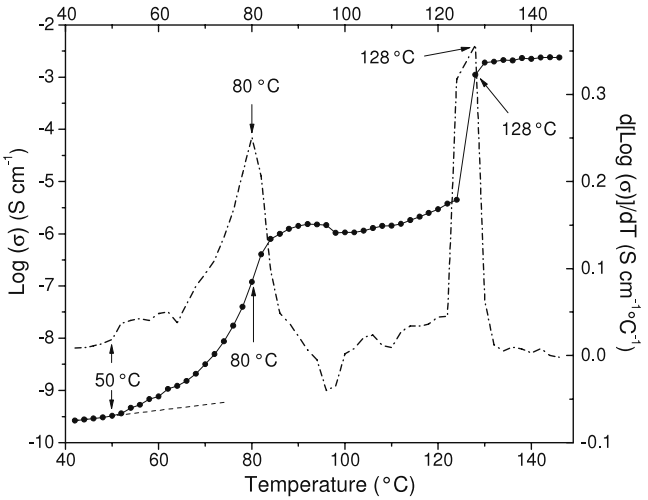

Figure 2. Temperature dependence of the conductivity ($\log \sigma$ versus T) of a dry fresh CHSe sample and its respective temperature derivative curve in the range of 40–150 °C. The average heating rate was fixed at 0.2 °C min^{-1}.

2. Experimental details

CHSe dry crystals were grown by slow evaporation from an aqueous solution, prepared by mixing stoichiometric amounts of caesium carbonate, Cs_2CO_3, and selenic acid H_2SeO_4 [16]. The sample was stored in a dissector with silica gel.

Simultaneous thermogravimetric and differential scanning calorimetric (TGA–DSC) measurements on two fresh CHSe samples were performed by using TA-Instruments SDT 2960 at 0.2 and 10 °C min^{-1} heating rates, respectively. Modulated (MDSC) and conventional differential scanning calorimetric (DSC) measurements were conducted on this salt with a TA-Instruments 2920 Analyzer. The MDSC measurements were made with an average heating rate of 0.2 °C min^{-1}, while the DSC ones were done on four fresh samples by using 0.2, 10, 35 and 75 °C min^{-1} heating rates, respectively. For all these experiments, the MDSC and SDT equipment was carefully calibrated for each heating rate, including temperature, enthalpy, onset slope (thermal resistance) and weight for the latter. The amplitude and period of the modulated temperature for the MDSC measurements were 0.2 °C and 60 s, respectively.

A flat single crystal with conducting silver paint on both faces was used as electrode for the complex impedance measurements, which were performed by means of a Solartron 1260 Analyzer. The dc conductivity was calculated from the frequency dependence of the real and imaginary part of the impedance plots in the complex plane by using an equivalent circuit fit. A flux of 50 ml min^{-1} of dry nitrogen gas (with water content of 1.5 ppm) was used as a purge gas during and before (one day) all these measurements. High temperature x-ray powder diffraction patterns at different isotherms (55, 90, 110, 120, 135 and 150 °C) were taken by using a Bruker-AXS D8 Advance x-ray diffractometer equipped with an Anton Paar HTK-1200 high temperature furnace. These data were obtained by using Kα radiation ($\lambda = 1.5406$ Å) with a 2θ scan step of 0.02° every 5 s.

3. Results and discussion

The temperature dependence of simultaneous weight and heat flow measurements performed on a dry fresh CHSe sample, heated at 0.2 °C min^{-1}, is plotted in figure 1. Taking into account that in this technique the TGA and DSC signals are responses from the same sample and that comparing the DSC (80.4, 84.4, 128.3 °C) and DTG (80.3, 84.3, 128.3 °C) temperature peaks, respectively, which are practically the same, we can firmly state that each of all these DSC endothermic peaks is associated with a weight loss step. The first and second DSC and DTG peaks are partially overlapped. It is also important to point out that at around the same temperature (50 °C) as the DTG curve starts to increase at, the DSC baseline slope starts to change.

Figure 2 shows the temperature dependence on the conductivity and its temperature derivative curve for a dry CHSe sample, heated at 0.2 °C min^{-1}. The conductivity curve presents two conductivity increase steps at around 80 and 128 °C. The temperature derivative of the conductivity curve shows two peaks. The peak temperatures of these are just the same peak temperatures as were measured for the first and third DSC and DTG peaks, respectively (see figure 1). The onset temperature of the first observed weight loss and DSC baseline slope change at 50 °C (see figure 1) also agrees closely with the first onset temperature of the conductivity increase (see figure 2).

For CHS, the endothermic effects and conductivity changes associated with the III $\rightarrow$ II and II $\rightarrow$ I phase transitions at 60 and 141 °C, respectively, were explained as consequences of chemical decomposition processes at or very near the sample surface following reaction (1) rather than structural phase transitions [31]. Then, as for the CHS case [31], since CHSe also presents weight loss steps at the same temperatures as endothermic effects and conductivity increase steps appear at, and because the physical and chemical

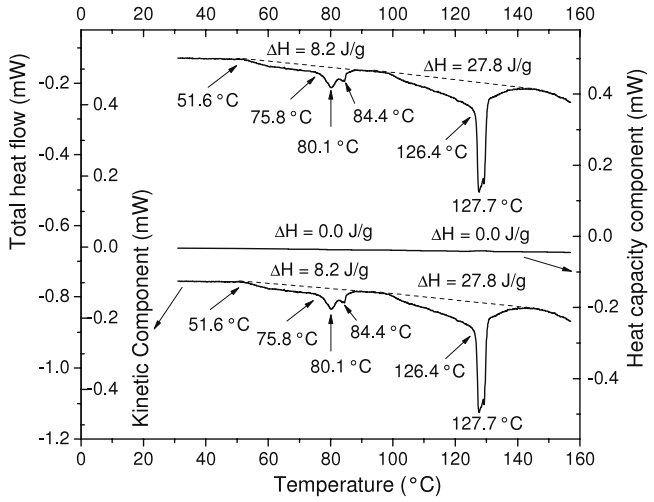

Figure 3. Total heat flow and its time-dependent (kinetic component) and time-independent (heat capacity component) components of a dry, wafer-shaped crystal, in the 30–160 °C temperature range. The heating rate was fixed at 0.2 °C min^{-1}.

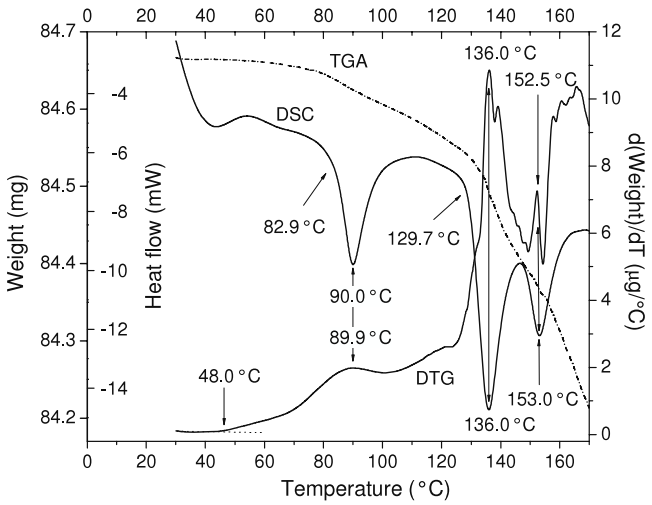

Figure 4. Simultaneous TGA–DSC measurements on a fresh dry CHSe sample in the 30–170 °C temperature range. The heating rate was fixed at 10 °C min^{-1}. The DTG curve corresponds to the temperature derivative of the TGA curve.

properties of CHSe and CHS are very similar, as we pointed out earlier, we propose the hypothesis that the III → II and II → I phase transitions close to 80 and 128 °C, respectively, for CHSe should be instead explained as consequences of two main chemical decomposition processes at or very near the CHSe sample surface at these temperatures, following the reaction

$$2CsHSeO_4 \rightarrow Cs_2Se_2O_7 + H_2O. \quad (2)$$

In agreement with these results, it is also suggested that the Brillouin spectroscopy observations [10, 11] at 50 °C, like the low onset temperature of the conductivity increase at about 50 °C (see figure 2), correspond to the low onset temperature of a chemical decomposition (following reaction (2)) accompanied by a weight loss at this temperature (see figure 1).

Even though it is clear that at around 80 and 128 °C weight loss steps agree well in temperature with the DSC endothermic peaks and conductivity increase steps, we should not discard the possibility that the III → II and II → I phase transitions could also occur simultaneously with the chemical decomposition on the sample surface. In this case, as these phase transitions are of the first-order type [14, 26] and as the chemical decomposition processes necessarily require energy to break molecular bonds (to generate chemical products), the enthalpy measured from the DSC peaks should be the sum of these contributions. The thermal results for a CHSe single crystal in the 30–160 °C temperature range obtained using the MDSC technique, which allows separation of the time-dependent (kinetic) component from the time-independent (heat capacity) component of the thermal response of the sample to a modulated heat flow [32], are shown in figure 3. These results indicate that the enthalpy associated with the thermal events at around 80 °C and 128 °C as measured from the kinetic component corresponds to the total enthalpy values measured (8.2 J g^{-1} and 27.8 J g^{-1}, respectively) from the total heat flow signal. Therefore, since the decomposition reactions are time-dependent phenomena, the results suggest that the total enthalpy of these thermal events should be exclusively associated with chemical processes.

Moreover, another classic experiment used to identify whether a thermal transformation of a compound is of physical or chemical nature is that in which one checks whether the temperature (and enthalpy) transformation changes when fresh samples are heated at different heating rates. Similar to the results presented in figure 1, those in 4 show the temperature dependence of simultaneous weight and heat flow signals for a dry fresh CHSe sample, but now using a heating rate of 10 °C min^{-1}.

Comparing figures 1 and 4, we see that the first and second DSC peaks overlap completely as their corresponding DTG peaks do; the third DTG peak is much better resolved. An additional DSC peak with its corresponding DTG peak is observed at around 153 °C, indicating that when CHSe is heated at 10 °C min^{-1} a new chemical decomposition event appears at this temperature value. By comparing these results, it can been seen that when heating rate is increased from 0.2 to 10 °C min^{-1}, the onset and the peak temperatures of the DSC peak associated with the III → II phase transition (the first one) shift upward by 6.6 and 9.6 °C, respectively; the onset and peak temperatures associated with the II → I phase transition shift upward by 3.7 and 8.0 °C, respectively; the weight loss steps, at around 80 and 128 °C, are also shifted upward by the same temperature interval as that of the DSC endothermic events (that is, the DSC (90, 136 °C) and the corresponding DTG (89.9, 136 °C) temperature peaks are the same, see figure 4). These observations constitute further evidence that the DSC endothermic events associated with the III → II and II → I phase transitions close to 80, and 128 °C should be entirely associated with chemical processes.

Additional thermal analysis on CHSe was also done by using the DSC Analyzer (TA-Instruments 2920) at four different heating rates: 0.2, 10, 35, and 75 °C min^{-1} (see figure 5).

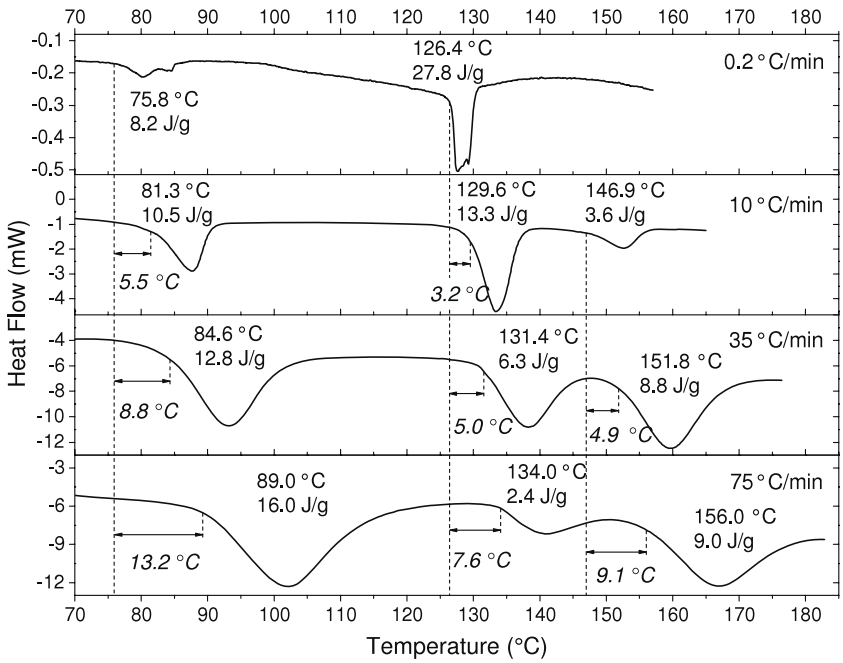

Figure 5. DSC thermograms of four fresh samples heated at 0.2, 10, 35, and 75 °C min^{-1}, respectively. The dotted vertical lines show the onset temperature at the lowest heating rate where the endothermic peaks appear. The double arrow shows the temperature interval where the onset temperature of each peak is shifted upward when the sample is exposed to different heating rates.

Checking these results, it can be stated that when the heating rate of fresh CHSe samples is progressively increased from 0.2 to 75 °C min^{-1} the onset temperature and enthalpy of the DSC peak associated with the III → II phase transition gradually increase from 75.8 to 89.0 °C and from 8.2 to 16.0 J g^{-1}, respectively (see figure 6). On the other hand, while the onset temperature of the DSC peak associated with the II → I phase transition progressively increases from 126.4 to 134.0 °C its respective enthalpies gradually decrease from 27.8 to 2.4 J g^{-1} (see figure 7). That is, the onset temperature and enthalpy of the DSC peak associated with the III → II phase transition increase by 13.2 °C and 7.8 J g^{-1} (95%), respectively; while the onset temperature of the DSC peak associated with the II → I phase transition increases by 7.6 °C and its corresponding enthalpy decreases by 25.4 (95%). Conversely, for the higher temperature peak that appears at higher heating rates (see figure 4), when this is increased from 10 to 75 °C min^{-1}, its onset temperature and enthalpy progressively increase from 146.9 to 156.0 °C and from 3.6 to 9.0 J g^{-1}, respectively. So, the onset temperature and the enthalpy increase by 9.1 °C and 4.6 J g^{-1} (250%), respectively.

Thus, the changes observed in the transformation temperatures and the corresponding enthalpy associated with the III → II and II → I phase transitions of CHSe when changing the heating rate (see figures 1 and 4–7) also show that they could be much better understood as a consequence of a chemical transformation rather than a physical one. Furthermore, these results are also supported by the MDSC analysis (see figure 3) in which the total enthalpy measured for the thermal events at around 80 and 128 °C corresponds exclusively to chemical processes, because otherwise the coexistence with physical transformations should be appearing

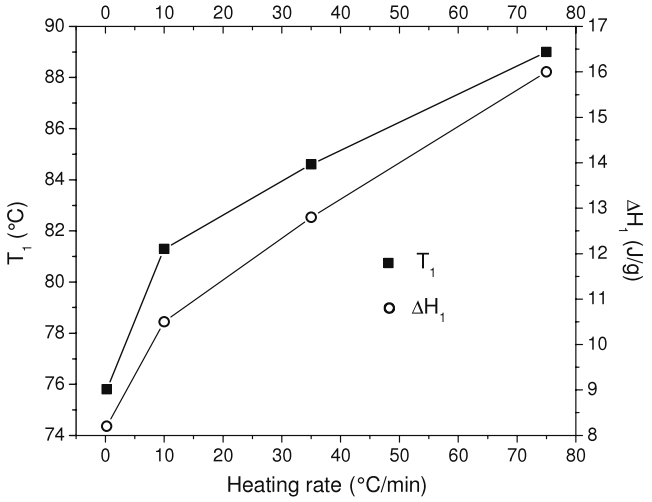

Figure 6. Heating rate dependence of the onset temperature, T_1, and enthalpy, ΔH_1, of the endothermic peak associated with the first phase transition (III → II) shown in figure 5.

as two additional DSC peaks at these fixed temperatures values, when the sample is heated at a high heating rate, for example at 75 °C min^{-1}, for which the DSC curve is shown in figure 5.

Figure 8 shows high temperature x-ray diffraction patterns of powdered CHSe at several isotherms from 55 to 150 °C. The 55 °C diffraction pattern is almost identical to that reported by Baran *et al* [8] for a monoclinic symmetry with space group $P2_1/c$ (phase III), except for the asterisk-marked peak, whose presence is still unexplained. Miller indices for the diffraction peaks were assigned according to reported data [8]. Comparing

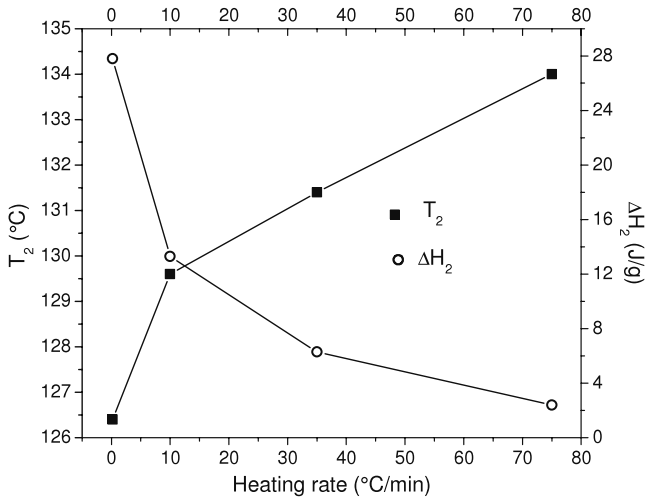

Figure 7. Heating rate dependence of the onset temperature, T_2, and enthalpy, ΔH_2, of the endothermic peak associated with the second phase transition (II → I) shown in figure 5.

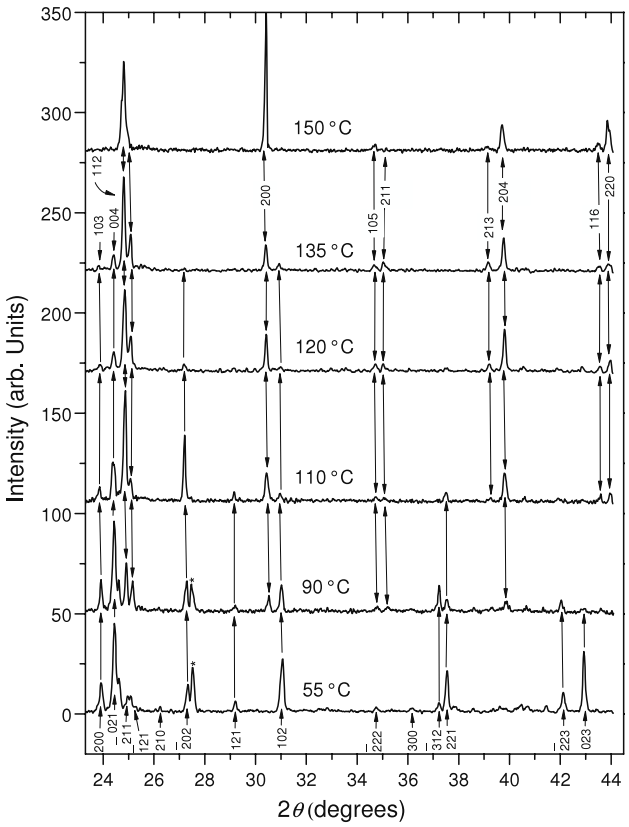

Figure 8. XRD patterns of CHSe dry powder at 55, 90, 110, 120, 135, and 150 °C, respectively. Miller indices assigned to the reflection peaks for the patterns obtained at 55 and 135 °C (and 175 °C) are like those assigned to phases III [8] and I (obtained from the cell parameters and space group of [7]), respectively. The peaks of phase III shown on the 55 °C pattern that remain on subsequent high temperature patterns and those new ones that appear on the 90–150 °C patterns are marked with single and double arrows, respectively. The asterisk-marked peak is probably due to an impurity trace.

the 90 °C to the 55 °C patterns, it is clear that they are not identical to each other, but the first one is a superposition of two x-ray spectra: a new one composed of peaks marked with double arrows and that of phase III, whose peaks are marked with single arrows. On further heating, it is observed in general that, while the intensity of phase III peaks progressively reduces, the intensity of the new peaks gradually increases, such that CHSe must be heated to 150 °C to get a spectrum composed of only the new peaks. A similar observation was made by Belushkin *et al* [16] and De Sousa *et al* [17] using neutron diffraction studies and infrared spectroscopy, respectively. In agreement with the latter workers [17], we do not believe that in the temperature range from 87 to 127 °C a coexistence of two CHSe phases is present, as the first affirms [16]. Since the CHSe transformations above room temperature have been identified as first-order phase transitions [14, 26], the DSC results (see figures 1, 3 and 4) would indicate that the coexistence of phases should be only possible at the phase transition temperatures (at 80 and 128 °C, respectively), contrary to the XRD results showing that peaks of the low temperature phase III are also present in the 90, 110, 120 and even 135 °C patterns. According to the tetragonal cell parameters and space group reported by Komukae *et al* [7] for phase I of CHSe, the Miller indices were assigned to the peaks of the 135 and 150 °C patterns. By checking the two lower peaks of all patterns, it can be seen that the (200) and (021) peaks of phase III could be wrongly indexed as (103) and (004) for phase I, respectively.

If the whole sample is reacting according to equation (2), then only 3.25% of its weight is required to reduce. From the TGA measurement in figure 1, it can be found that at 90, 135, and 150 °C at least 5, 20, and 30% of the sample, respectively, should be $Cs_2Se_2O_7$. Now, since the sample used for the x-ray diffraction analysis is powdered, these percentages should be higher. We believe that the 90 °C diffractogram in figure 8 may correspond to a sample with a composition of two solid phases: the CHSe phase III and $Cs_2Se_2O_7$, which appears as a segregated substance at the surface of the CHSe grains, and whose x-ray pattern overlaps with that of CHSe phase III at this temperature. If CHSe is further heated, more and more $Cs_2Se_2O_7$ grows over the sample surface. This explains why the intensity of the new spectral peaks increases while the intensity of phase III peaks decreases. Although the remaining sample at 150 °C may still contain some of the CHSe phase, only $Cs_2Se_2O_7$ adsorbs the whole x-ray energy and the spectrum at this temperature corresponds just to that of $Cs_2Se_2O_7$. Consequently, these results confirm that the III → II and II → I phase transitions do not take place. However, if this interpretation were to be wrong, then, since the 120 and 135 °C patterns are essentially the same, it is logical to conclude that the II → I phase transition does not take place. Moreover, the previously reported IR observation [17] that (upon heating the salt through the 80–128 °C temperature range) while the dielectric strength of the phase III modes abruptly falls to 128 °C, the emergent mode situated at 670 cm^{-1} behaves in the opposite manner, as well as the reported CHSe two-phase coexistence [16], could have the same explanation as we have offered here for our x-ray data.

As for the CHS [31] and KH_2PO_4 family compounds [33], we believe that in CHSe the kinetic course of the proposed solid state decomposition (equation (2)) is dominated by the initiation of localized reactions at particular localities and the subsequent advancement of a reactive interface into the non-decomposed reactant. This initiation occurs at, or very near, the crystal external surface at sites where crystallographic disorder exists. The crystal quality of the surface could be different depending on its defect species, density, and distribution of the nucleation sites. Therefore, this phenomenon could explain why the reported III → II (50–97 °C) and II → I (124–131 °C) phase transition temperatures are so widespread in literature.

We believe that when CHSe is heated from room temperature, at around 50 °C a very early initiation of decomposition starts to manifest, reaching the highest rate of the first stage of decomposition around 80 °C. The observed first increase of the CHSe conductivity [1] is due to the presence of water at the surface of the salt, formed according to reaction (2), which dissolved part of it. After this reaction takes place, initially at the most external surface layer, the resultant water is partially evaporated and a thin solid crust of $Cs_2Se_2O_7$ covers the sample surface. Therefore, electrical conductivity increases to around 10^{-6} S cm^{-1}. If now the sample were cooled down, the reverse reaction

$$Cs_2Se_2O_7 + H_2O \rightarrow 2CsHSeO_4 \qquad (3)$$

would not take place, since the reverse DSC peak is not shown, probably because water is not sufficiently available either at the surface or in the surrounding atmosphere. In fact, only when the sample previously heated above 82 °C is exposed to a moist atmosphere at room temperature, and/or when removing the solid $Cs_2Se_2O_7$ crust formed on the sample surface by grinding it in a mortar, is the DSC peak at 82 °C shown again on the subsequent heating run [14, 18]. By comparing observations of Belushkin *et al* [16], that when CHSe is cooled from 152 °C down to room temperature, the two-phase system persists even if it is annealed at this temperature for four weeks, to those of Colomban *et al* [22], that if CHSe is cooled from phase II or I down to room temperature, phase I can be obtained by annealing at this temperature from three hours to many days, we believe that the differences in these observations are a consequence of the difference in relative humidity value of their respective laboratory environments.

Upon heating CHSe from 80 °C, the solid $Cs_2Se_2O_7$ crust partially hindered the progress of the reaction, but when the salt reaches 128 °C the highest rate of the second stage of decomposition takes place, so reaction (2) continues its propagation inside the sample (below the already formed $Cs_2Se_2O_7$ crust) forming a water–liquid phase. We believe that, following the same scheme as was proposed for the H_2O–$Cs_2S_2O_7$–$CsHSO_4$ system, where a water phase is strongly bonded to $Cs_2S_2O_7$ [31], an identical phenomenon occurs in the H_2O–$Cs_2Se_2O_7$–$CsHSeO_4$ system. So, although part of the water is released on heating the sample through 128 °C, as indicated by the TGA measurements (see figures 1 and 4), some portion remains in the sample such that it is used for the hydrolysis according to reaction (3), occurring during the subsequent cooling run. In fact, the MDSC cooling curve

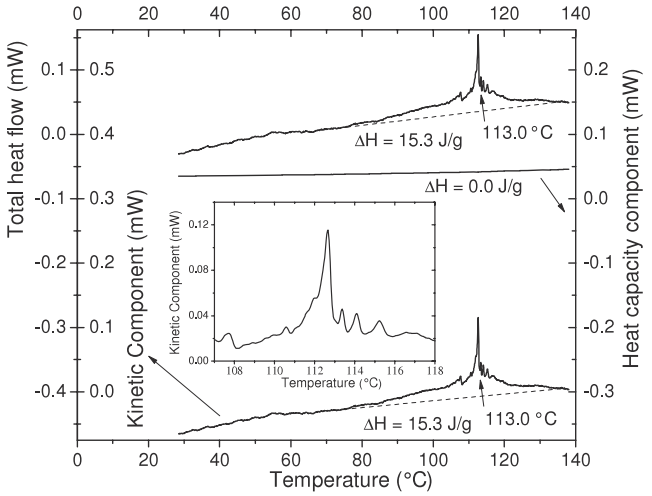

Figure 9. Total heat flow and its time-dependent (kinetic component) and time-independent (heat capacity component) components, for a cooling cycle from 140 to 28 °C, for a sample that was previously heated up to 145 °C. The heating and cooling rates used were 0.2 °C min^{-1}. The inset shows an amplification for the kinetic component in the 107–118 °C temperature range.

recorded at a rate of 0.2 °C min^{-1} (see figure 9) shows several exothermic peaks at around 113 °C with a total enthalpy of 45% less than that of the endothermic peak observed in the first heating run. The presence of this series of several exothermic peaks and the fact that the kinetic enthalpy component of these anomalies corresponds to the total enthalpy value measured from the total heat flow signal favour the hypothesis that when CHSe is cooling down from some temperature degrees above 128 °C, a sequence of chemical transformations in different sample regions (following reaction (3)) at around 113 °C take place, rather than physical transformations [5, 12, 13, 20, 22].

The proposed scheme for the phase behaviour of CHSe could explain its high conductivity above 128 °C, assuming that over the surface of the salt the H_2O–$Cs_2Se_2O_7$ system behaves as a proton-conducting polymer electrolyte membrane: the water dissolves part of the salt, providing protons to be conducted through the water embedded in the polymer (dimer) matrix. Moreover, this point of view could explain both the observation that an important contribution to the conductivity of phase I corresponds to Cs^+ ions [13] and the existence of mobile protons below T_c [27, 28]. Additionally, the unusual colour patterns observed [21] for phase I could also be understood through the refraction of the polarized light on the water near the sample surface. Therefore, our results support the concept that the CHSe phase above 128 °C is not a superprotonic conducting phase.

4. Conclusion

In summary, from our phase interrelationship study on CHSe, based on our simultaneous TGA–DSC, MDSC, DSC, impedance analyses, and x-ray diffraction, we propose that the high temperature phenomena observed for this acid salt could be explained by a thermal dehydration like the reaction (equation (2)) taking place upon heating above

room temperature. In consequence, the endothermic effects and conductivity changes associated previously with phase transitions in CHSe: phase transition III → II [5, 10–14, 28] and the phase transition to a superprotonic conducting phase [5–7, 16, 17, 20, 21, 27, 28] (phase transition II → I) around 80 and 128 °C, respectively, could be due to chemical decomposition processes at or near the surface of the specimen.

Acknowledgments

This work was financed by the International Programme in the Physical Sciences, IPPS, of Uppsala University, Sweden; the Colombian Research Agency, COLCIENCIAS, and the Excellence Centre for Novel Materials, CENM.

References

[1] Norby T 2001 *Nature* **410** 877–8
[2] Haile S M, Boysen D A, Chisholm C R I and Merle R B 2001 *Nature* **410** 910–3
[3] Uda T, Boysen D A and Haile S M 2005 *Solid State Ion.* **176** 127–33
[4] Chisholm C and Haile S M 2007 *US Patent Specification* 7,255,962
[5] Baranov A I, Shuvalov L A and Shchagina N M 1982 *JETP Lett.* **36** 459–62
[6] Baranov A I, Merinov B V, Tregubchenko A V, Khiznichenko V P, Shuvalov L A and Shchagina N M 1989 *Solid State Ion.* **36** 279–82
[7] Komukae M, Tanaka M, Osaka T, Makita Y, Kozawa K and Uchida T 1990 *J. Phys. Soc. Japan* **59** 197–206
[8] Baran J and Lis T 1987 *Acta Crystallogr.* C **43** 811–3
[9] Belushkin A V, Adams M A, Hull S and Shuvalov L A 1995 *Solid State Ion.* **77** 91–6
[10] Luspin Y, Vaills Y and Hauret G 1995 *Solid State Ion.* **80** 277–81
[11] Luspin Y, De Sousa Meneses D and Simon P 2000 *Solid State Commun.* **114** 361–4
[12] Pham-Thi M, Colomban Ph, Novak A and Blinc R 1985 *Solid State Commun.* **55** 265–70
[13] Colomban Ph, Pham-Thi M and Novak A 1986 *Solid State Ion.* **20** 125–34
[14] Baranowski B, Friesel M and Lundén A 1986 *Z. Naturf.* a **41** 981–2
[15] Belushkin A V, Carlile C J and Shuvalov L A 1992 *J. Phys.: Condens. Matter* **4** 389–98
[16] Belushkin A V, Natkaniec I, Pakida N M, Shuvalov L A and Wasicki J 1987 *J. Phys. C: Solid State Phys.* **20** 671–87
[17] De Sousa Meneses D, Simon P and Luspin Y 2000 *Phys. Rev.* B **61** 14382–8
[18] Friesel M, Lundén A and Baranowski B 1989 *Solid State Ion.* **35** 91–8
[19] Lundén A, Baranowski B and Friesel M 1991 *Ferroelectrics* **124** 103–7
[20] Blinc R, Dolinšek J, Lahajnar G, Zupančič I, Shuvalov L A and Baranov A I 1984 *Phys. Status Solidi* b **123** K83–7
[21] Baranov A I, Fedoshuk R M, Schagina N M and Shuvalov L A 1984 *Ferroelectr. Lett. Sect.* **2** 25–8
[22] Colomban Ph 1987 *J. Mol. Struct.* **161** 1–14
[23] Foose D and Mitra G 1977 *J. Inorg. Nucl. Chem.* **39** 553–4
[24] Yokota S 1982 *J. Phys. Soc. Japan* **51** 1884–91
[25] Balagurov A M, Beskrovnyi A I, Dutt I D, Shuvalov L A and Schagina N M 1986 *JINNR (Dubna, USSR)* Communication P14-86-39
[26] Friesel M, Baranowski B and Lundén A 1989 *Solid State Ion.* **35** 85–9
[27] Yoshida Y, Matsuo Y and Ikehata S 2005 *Solid State Ion.* **176** 2457–60
[28] Yoshida Y, Hisada K, Matsuo Y and Ikehata S 2008 *Solid State Ion.* **178** 1869–71
[29] Simon A and Wagner H 1961 *Z. Anorg. Allgem. Chem.* **311** 102–9
[30] Walrafen G E, Irisii D E and Young T F 1962 *J. Chem. Phys.* **37** 662
[31] Ortiz E, Vargas R A and Mellander B-E 2006 *J. Phys.: Condens. Matter* **18** 9561–73
[32] Reading M, Elliott D and Hill V 1992 *Proc. 21st North American Thermal Analytical Society (Atlanta, GA)* pp 145–50
[33] Lee K S 1996 *J. Phys. Chem. Solids* **57** 333–42